The Journal of Immunology

Talin1 Methylation Is Required for Neutrophil Infiltration and Lipopolysaccharide-Induced Lethality

Thomas Jun Feng Lim and I-Hsin Su

J Immunol 2018; 201:3651-3661; Prepublished online 12 November 2018;
doi: 10.4049/jimmunol.1800567
http://www.jimmunol.org/content/201/12/3651

The Journal of Immunology is published twice each month by
The American Association of Immunologists, Inc.,
1451 Rockville Pike, Suite 650, Rockville, MD 20852

Print ISSN: 0022-1767 Online ISSN: 1550-6606.

Talin1 Methylation Is Required for Neutrophil Infiltration and Lipopolysaccharide-Induced Lethality

Thomas Jun Feng Lim and I-Hsin Su

Talin1, a well-established integrin coactivator, is critical for the transmigration of neutrophils across the vascular endothelium into various organs and the peritoneal cavity during inflammation. Several posttranslational modifications of talin1 have been proposed to play a role in this process. In this study, we show that trimethylation of talin1 at Lys2454 by cytosolic Ezh2 is substantially increased in murine peritoneal neutrophils upon induction of peritonitis. By reconstituting talin1-deficient mouse myeloid cells with wild-type, methyl-mimicking, or unmethylatable talin1 variants, we demonstrate that methylation of talin1 at Lys2454 is important for integrin-dependent neutrophil infiltration into the peritoneal cavity. Furthermore, we show that treatment with an Ezh2 inhibitor or reconstitution of talin1-deficient myeloid cells with unmethylatable talin1 significantly reduces the number of organ-infiltrating neutrophils and protects mice from LPS-induced mortality. *The Journal of Immunology*, **2018, 201: 3651–3661.**

Cell adhesion and migration processes are highly dynamic and require temporal and spatial coordination of a large number of cytosolic and transmembrane proteins. For example, the recruitment of neutrophils to sites of infection, which is essential for pathogen clearance (1), is initiated by selectin-mediated rolling of neutrophils along postcapillary venules, where P-selectin glycoprotein-1 (CD162) expressed on the surface of neutrophils interacts with constitutively expressed selectins on the surface of endothelial cells (2–4). This process of neutrophil rolling promotes the interaction of chemokine receptor CXCR2 expressed on the surface of neutrophils with endothelial cell–bound chemokine CXCL1, thereby triggering a CXCR2-dependent signaling cascade that eventually leads to the activation of LFA-1 (a dimer of β_2-integrin and integrin αL) in a talin1-dependent manner (5). Talin1 binding to the membrane proximal NPxF motif and the membrane proximal region of the β_2-integrin tail induces structural changes in the LFA-1 integrin heterodimer in neutrophils, converting it from a low-affinity state to an active configuration with high binding affinity for ICAM-1, a ligand expressed on the surface of endothelial cells (2). Recruitment of kindlin3 to the membrane distal NxxF motif of β_2-integrin reinforces the high affinity integrin/ligand interaction (5, 6) and ultimately leads to neutrophil arrest on the endothelial wall. Arrested neutrophils then initiate transmigration through the activation of Mac-1 (αMβ2) and spread and crawl toward endothelial cell junctions (paracellular migration route) or directly across endothelial cells (transcellular migration route) for entrance to tissues (7).

Proteins involved in the process of neutrophil migration are typically regulated by protein/protein interactions and/or posttranslational modifications (PTMs) that include phosphorylation, acetylation, ubiquitination, or proteolytic cleavage (8–11). Talin, the intermediate molecule that links integrins to the actin cytoskeleton, is perhaps the molecule with the best-defined role in regulating cell migration. It consists of a talin N-terminal head domain (THD), with a high-affinity binding site for the integrin β subunit, that is connected via an unstructured linker to a long C-terminal rod domain consisting of 13 helical bundles (R1–R13) (12). In the cytosol, talin adopts an autoinhibitory configuration through the formation of intramolecular interactions between the THD and the R9 domain (12–15). For talin activation, various proteins and molecules have been shown to be involved. For example, the interaction of Rap1/GTP-interacting adaptor molecule (RIAM) with the talin rod domain releases talin from its autoinhibitory conformation (16). Kank2 can also bind talin in the vicinity of its actin-binding site 2 (ABS2), keeping it in an activated state at focal adhesion (FA) belts while simultaneously reducing F-actin binding and traction force transmission to promote FA disassembly (17) or the formation of fibrillar adhesions (18, 19). Moreover, Skap2 can form a complex with Wiskott–Aldrich syndrome protein (WASp) to promote global actin polymerization and the binding of talin1 and kindlin3 to integrin, thereby regulating integrin activation and neutrophil recruitment in vivo (20). It has also been shown that negatively charged phosphatidylinositol-4,5-bisphosphate [PI(4,5)P2] at FAs may enable the activation of talin (13). Upon activation, talin can be regulated by calpain-mediated cleavage, followed by ubiquitination or arginylation (21–24). Turnover of leukocyte FAs requires proteasomal degradation of ubiquitinated THD, a process that is antagonized by cyclin-dependent kinase 5 (CDK5)–mediated phosphorylation of Ser425 in the THD (22). Arginylation of talin has also recently been reported to be essential for cell/cell adhesion (23). Additional PTMs may further alter talin function to influence cell migration. Indeed, our recent reports suggest a critical role for talin1 methylation in the regulation of adhesion dynamics and tumorigenesis (25, 26). We have shown that histone

School of Biological Sciences, College of Science, Nanyang Technological University, Singapore 637551, Republic of Singapore

ORCID: 0000-0002-5894-9580 (I-H.S.).

Received for publication April 23, 2018. Accepted for publication October 15, 2018.

This work was supported by the Agency for Science, Technology and Research Graduate Scholarship (to T.J.F.L.). This work was supported by the following Singapore Ministry of Education, Singapore Ministry of Health, and National Medical Research Council grants: Academic Research Fund Tier 1 RG40/13 and RG36/17, MOE2013-T2-2-038, MOE2017-T2-2-054, and NMRC-CBRG/0057/201 (to I-H.S.).

Address correspondence and reprint requests to Prof. I-Hsin Su, Nanyang Technological University, 60 Nanyang Drive, Singapore 637551, Republic of Singapore. E-mail address: ihsu@ntu.edu.sg.

Abbreviations used in this article: ABS3, actin-binding site 3; BALF, bronchoalveolar lavage fluid; BM, bone marrow; BSS, balanced salt solution; BUN, blood urea nitrogen; EV, empty vector; Ezh2, enhancer of zeste homolog 2; FA, focal adhesion; K2454me3, Ezh2-mediated trimethylation of talin1 at Lys2454; MHCII, MHC class II; PTM, posttranslational modification; THD, talin N-terminal head domain.

methyltransferase enhancer of zeste homolog 2 (Ezh2)–mediated trimethylation of talin1 at Lys2454 (K2454me3) in the actin-binding site 3 (ABS3) disrupts the binding of F-actin to talin1, leading to enhanced calpain-dependent cleavage of talin1 and elevated adhesion turnover (25, 26).

Because the distribution of leukocytes and, in particular, the extravasation of neutrophils into sites of infection or inflammation is largely dependent upon integrin activation, we sought to determine the physiological significance of talin1 methylation in vivo. Our results showed that talin1/K2454 trimethylation in peritoneal neutrophils was induced in vivo during the progression of peritonitis. The importance of this methylation in regulating neutrophil infiltration into the peritoneal cavity and LPS-induced mortality was further demonstrated in chimeric mice with neutrophils expressing talin1 methylation variants and mice treated with an Ezh2 inhibitor. Our studies indicate that Ezh2-mediated talin1/K2454me3 controls the migration of neutrophils and possibly other immune cells under various disease conditions, resulting in broad impacts on overall immune responses.

Materials and Methods

Mice

Tln1$^{f/f}$ mice (27) were crossed with *LysM*-Cre mice (28) to generate mice with talin1-deficient myeloid cells. All mice were bred and maintained under specific pathogen-free conditions at the animal facility of the School of Biological Sciences, Nanyang Technological University. All mouse protocols were conducted in accordance with the guidelines of the Nanyang Technological University Institutional Animal Care and Use Committee.

Organ collection and preparation

Organ collection and preparation was carried out as previously described (25). Peritoneal cells were collected by peritoneal lavage using 5 ml ice-cold RPMI 1640 medium or balanced salt solution (BSS) (29) supplemented with 2% FCS. Bronchoalveolar lavage fluid (BALF) was collected according to the standard protocol. Single-cell suspensions were generated and stained for flow cytometry analysis.

Production of retroviral supernatants

To produce retroviral supernatants for the transduction of bone marrow (BM) stem cells, HEK-293T cells were transfected with 10 μg MIG/GFP empty vector (EV), MIG/GFP wild-type talin1 (K2454), MIG/GFP/talin1/K2454F, MIG/GFP/talin1/K2454A, MIG/GFP/talin1/K2454Q, or MIG/GFP/talin1/W359A, along with 10 μg pCL-Eco retrovirus packaging plasmid. Virus-containing supernatants were collected at 48 and 72 h and filtered (0.45 μm) (Pall) before spin transduction of target cells (see below).

Generation of BM chimeras

Tln1$^{f/f}$*LysM*-Cre mice were i.p. injected with 5-fluorouracil (150 mg/kg) (Sigma-Aldrich) and sacrificed 4 d later. BM cells from *Tln1*$^{f/f}$*LysM*-Cre mice were harvested and erythrocytes lysed. Subsequently, BM cells were cultured on fibronectin-coated (10 μg/ml) (Sigma-Aldrich) six-well plates (Thermo Fisher Scientific) in complete RPMI 1640 medium (with 10% FCS, 55 μM 2-ME, 100 U/ml penicillin/streptomycin, and 2 mM L-glutamine) (Life Technologies) supplemented with 6 ng/ml IL-3, 10 ng/ml IL-6, and 10 ng/ml stem cell factor (all from PeproTech) for 2 d before transduction. BM cells were transduced twice (on day 2 and 3) with retrovirus supernatant containing 5 μg/ml polybrene (Sigma-Aldrich) at 1000 × *g* for 1.5 h to express N-terminal GFP-fused wild-type talin1 (K2454) or talin1 variants (talin1/K2454F, K2454A, and K2454Q). EV was used as control. After two rounds of transduction, transduced BM cells were FACS-sorted for GFP expression and cultured for two to three more days before adoptive transfer (5×10^5 GFP$^+$ BM stem cells) into lethally irradiated (5.5 Gy × 2) CD45.1 congenic wild-type mice. Reconstituted BM chimeric mice were fed with water containing antibiotics for 2 wk before analysis 8 wk later.

Abs and reagents

The following Abs for flow cytometry analysis were used: CD45/APC/Cy7 (30-F11), CD45.2/APC (104), Ly6G/PE (1A8), CD11b/BV605 (M1/70), CD11b/BUV395 (M1/70), F4/80/biotin (BM8), streptavidin/PeCy7, Ly6C/FITC (HK1.4), MHC class II (MHCII)/PeCy5 (M5/114.15.2), MHCII/Pacific Blue (M5/114.15.2), and anti-GFP (FITC) (ab6662) (all from BioLegend, except CD11b/BUV395 from BD Biosciences and anti-GFP FITC–conjugate Ab from Abcam). Intracellular staining was performed using BD Cytofix/Cytoperm Kit (BD Biosciences) according to manufacturer's instructions. Topro3 (Invitrogen) and Live/Dead Fixable Violet dye (Thermo Fisher Scientific) were used to exclude dead cells. The following Abs for immunoprecipitation and Western blot were used: Talin (8D4; Sigma-Aldrich), CD29 (12G10; Abcam), CD11b (ab133357; Abcam), GFP (B-2; Santa Cruz Biotechnology), GAPDH (AM4300; Thermo Fisher Scientific), Vav1 (no. 2502), and Ezh2 (D2C9) Abs (both from Cell Signaling Technology). Talin1/K2454me3 custom Ab (25) was generated by YenZym Abs (San Francisco, CA). Evans blue dye was prepared according to the manufacturer's instructions (Sigma-Aldrich).

Immunoprecipitation

Peritoneal or BM neutrophils were purified (Miltenyi Biotec) at different time points and lysed in lysis buffer (20 mM HEPES, 1.5 mM EDTA, 2 mM $MgCl_2$, 150 mM NaCl, and 1% Triton X-100) supplemented with 1% protease inhibitor mixture, 5 mM Na_3VO_4, 5 mM NaF, 1 mM DTT, and 1 mM PMSF (all from Sigma-Aldrich). Lysates were centrifuged at 16,000 × *g* for 10 min at 4°C. The supernatant was collected and precleared with Protein G Sepharose beads (GE Healthcare) for 30 min at 4°C. Anti-talin Ab was added to the lysates and incubated overnight at 4°C. Protein G Sepharose beads were added to the supernatant for 3–4 h at 4°C. Beads were washed three times in lysis buffer and boiled in 2× loading buffer. Immunoprecipitation of talin1 or GFP/talin1 from HEK-293T cells was performed in a similar fashion.

Induction of peritonitis and vascular permeability analysis

Mice were i.p. injected with 1 ml of 4% thioglycolate broth, fMLF (50 ng/mouse), or various doses of zymosan A (all from Sigma-Aldrich) to induce sterile peritonitis. Mice were sacrificed at the indicated time points upon induction of peritonitis. Peritoneal cells were collected with 5 ml BSS (29) containing 2% FCS and stained for flow cytometry analysis. To analyze vascular permeability, 100 μl Evans blue dye (30 mg/kg) (Sigma-Aldrich) was i.v. administered 30 min before inducing peritonitis. Peritoneal cells were collected with 5 ml BSS (29) containing 2% FCS and were pelleted, and the OD_{640} of the peritoneal fluid (supernatant) was used as a determinant of Evans blue leakage into the peritoneal cavity. For experiments involving the Ezh2 inhibitor GSK126 (Active Biochem), experimental mice were i.p. injected with 10 mg/kg of inhibitor 48 and 1 h prior to induction of peritonitis with 15 mg/kg body weight of LPS (O55:B5) (Sigma-Aldrich).

LPS-induced endotoxemia

Mice were i.p. injected with 15 mg/kg of body weight of LPS (O55:B5) (Sigma-Aldrich). Organs were collected from LPS-injected mice 20−24 h later, and single-cell suspensions were generated as previously described (25). Cells were subsequently stained for flow cytometry analysis.

ELISA

Peripheral blood was collected from mice 20−24 h after i.p. injection of LPS or PBS. Blood leukocytes were removed by centrifugation, and the amount of blood urea nitrogen (BUN) and creatinine was quantified using specific ELISA kits (Thermo Fisher Scientific and Cayman Chemical).

Statistical analysis

Two-tailed Student *t* test was performed to obtain *p* value for most of the statistical analysis shown in figures. Mantel–Cox log-rank test was used to determine the significant changes in Kaplan–Meier survival analysis. Figures were prepared using GraphPad Prism 7 (GraphPad Software). A *p* value < 0.05 was considered significant as indicated by $*0.01 < p < 0.05$, $**0.005 < p < 0.01$, and $***p < 0.005$.

Results

Talin1 is not required for the generation of innate immune cells

To study the functional roles of talin1 in innate immune cells, we analyzed neutrophils and macrophages from control (*Tln1*$^{f/f}$) and *Tln1*$^{f/f}$*LysM*-Cre mice in which the *loxP*-flanked *Tln1* allele (*Tln1*$^{f/f}$) was conditionally deleted in myeloid-lineage cells. Our results showed that talin1 was dispensable for the generation of neutrophils (Fig. 1A, 1B) and macrophages (Fig. 1C, 1D) in vivo. However, we detected an elevated number of talin1-deficient (*Tln1*$^{f/f}$*LysM*-Cre) neutrophils in the blood (Fig. 1A, 1B), which is likely due to reduced

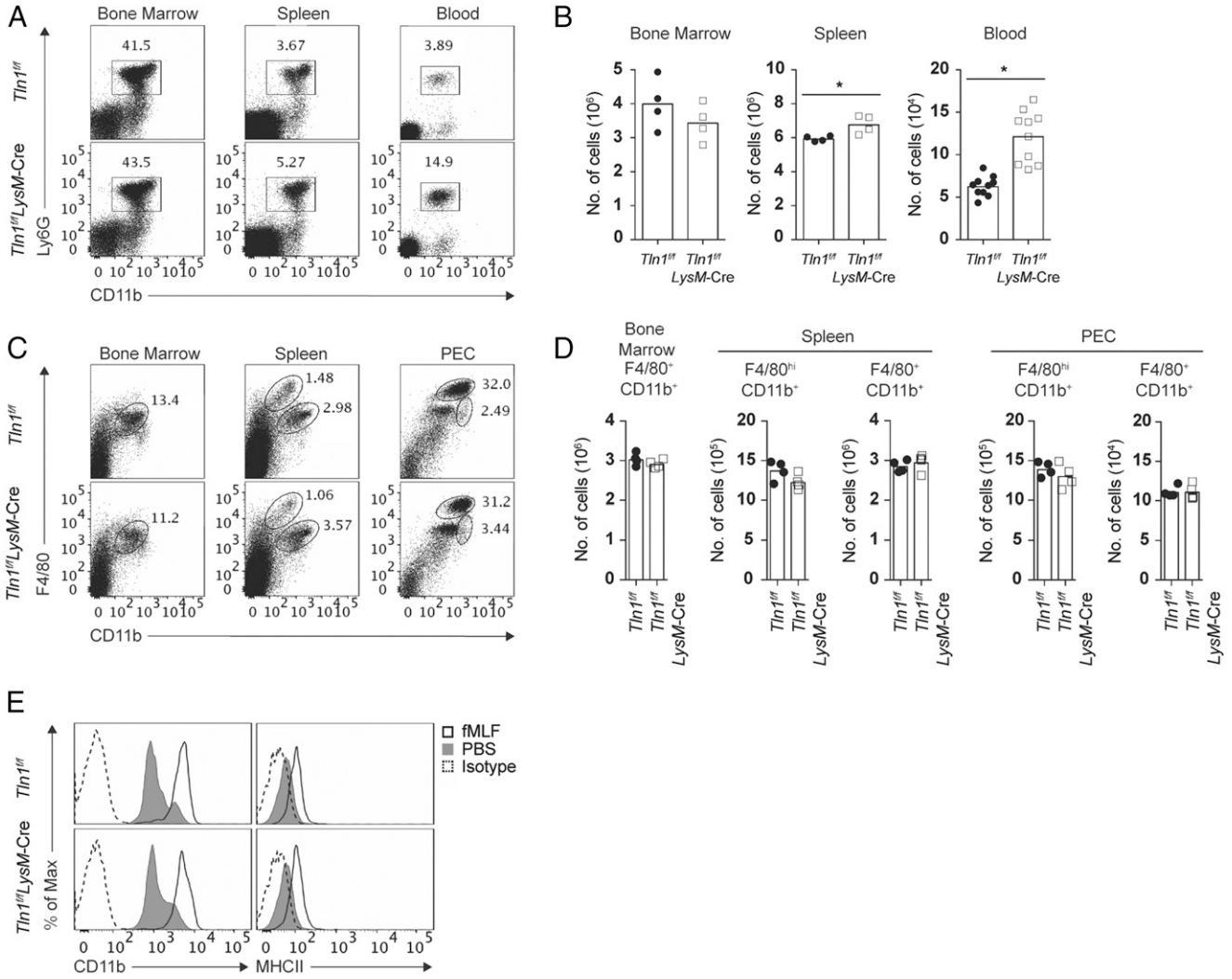

FIGURE 1. Characterization of talin1-deficient neutrophils and macrophages. (**A**) Representative dot plots of $Ly6G^+CD11b^+$ neutrophils isolated from the BM, spleen, and blood of control (*Tln1$^{f/f}$*) and *Tln1$^{f/f}$LysM*-Cre mice. (**B**) Absolute numbers of neutrophils were calculated based on the total cell numbers and the percentages of neutrophils ($n = 4$ per genotype [BM, spleen, and peritoneal cavity (PEC)] and 10 per genotype [blood]), as determined by flow cytometry (A). (**C**) Representative dot plots of macrophages from the BM, spleen, and PEC of control (*Tln1$^{f/f}$*) and *Tln1$^{f/f}$LysM*-Cre mice. (**D**) Absolute numbers of macrophages were calculated based on the total cell numbers and the percentages of macrophages ($n = 4$ per genotype [BM, spleen, and PEC]), as determined by flow cytometry (C). (**E**) Histograms of flow cytometry results show the expressions of CD11b and MHCII on wild-type and talin1-deficient neutrophils upon i.p. injection of fMLF ($n = 3$ mice per genotype). Each data point in the scatter bar graphs indicates the cell number from one experiment (B and D). The data shown was pregated on singlet, live cells (A and C), then $Ly6G^+CD11b^+$ neutrophils (A, B, and E) or the indicated macrophages (C and D) were further analyzed. The dot blots (A and C) and histograms (E) are representative of three to four independent experiments. $*0.01 < p \leq 0.05$.

steady state integrin-dependent extravasation of neutrophils into interstitial tissues, a process that requires functional talin1 (5). The modest elevation of neutrophil numbers in the spleens of *Tln1$^{f/f}$LysM*-Cre mice could also reflect the increased numbers of neutrophils in the blood circulation (Fig. 1B). Next, we stimulated control and *Tln1*-deleted neutrophils with the chemotactic peptide fMLF and found that both wild-type and talin1-deficient neutrophils were activated, as determined by the upregulation of surface CD11b and MHCII expression (30, 31) (Fig. 1E). Collectively, these data show that talin1 is dispensable for the generation of neutrophils and macrophages in vivo and does not play a significant role in the upregulation of MHCII and integrin upon activation.

Talin1 is crucial for the recruitment of neutrophils during peritonitis

Because the infiltration of neutrophils across the peritoneum is an integrin-dependent process (2, 32), talin1 deficiency is likely to affect the recruitment of neutrophils during inflammation. Therefore, we induced sterile peritonitis in mice by i.p. injection of thioglycolate or fMLF to examine the integrin-dependent migration of neutrophils into the peritoneal cavity. Although the numbers of wild-type and talin1-deficient neutrophils in the peritoneal cavity were low and comparable under steady state conditions (Fig. 2A–D), significantly higher numbers of wild-type neutrophils, compared with talin1-deficient neutrophils, were recruited to the peritoneal cavity at all time points after thioglycolate (Fig. 2A, 2B) or fMLF administration (Fig. 2C, 2D). This result was expected, because talin is known to be essential for the extravasation of leukocytes through endothelial cells (2, 4). However, we also noticed that fMLF elicited modest increases in the numbers of infiltrating talin1-deficient peritoneal neutrophils compared with the numbers of cells recruited by thioglycolate (Fig. 2A–D). These results correlated with slightly elevated vascular leakage, as indicated by the higher amount of Evans blue dye in the peritoneal fluid of mice injected with fMLF, compared with thioglycolate (Fig. 2E, 2F). These results support the general consensus that talin is essential for integrin-dependent cell

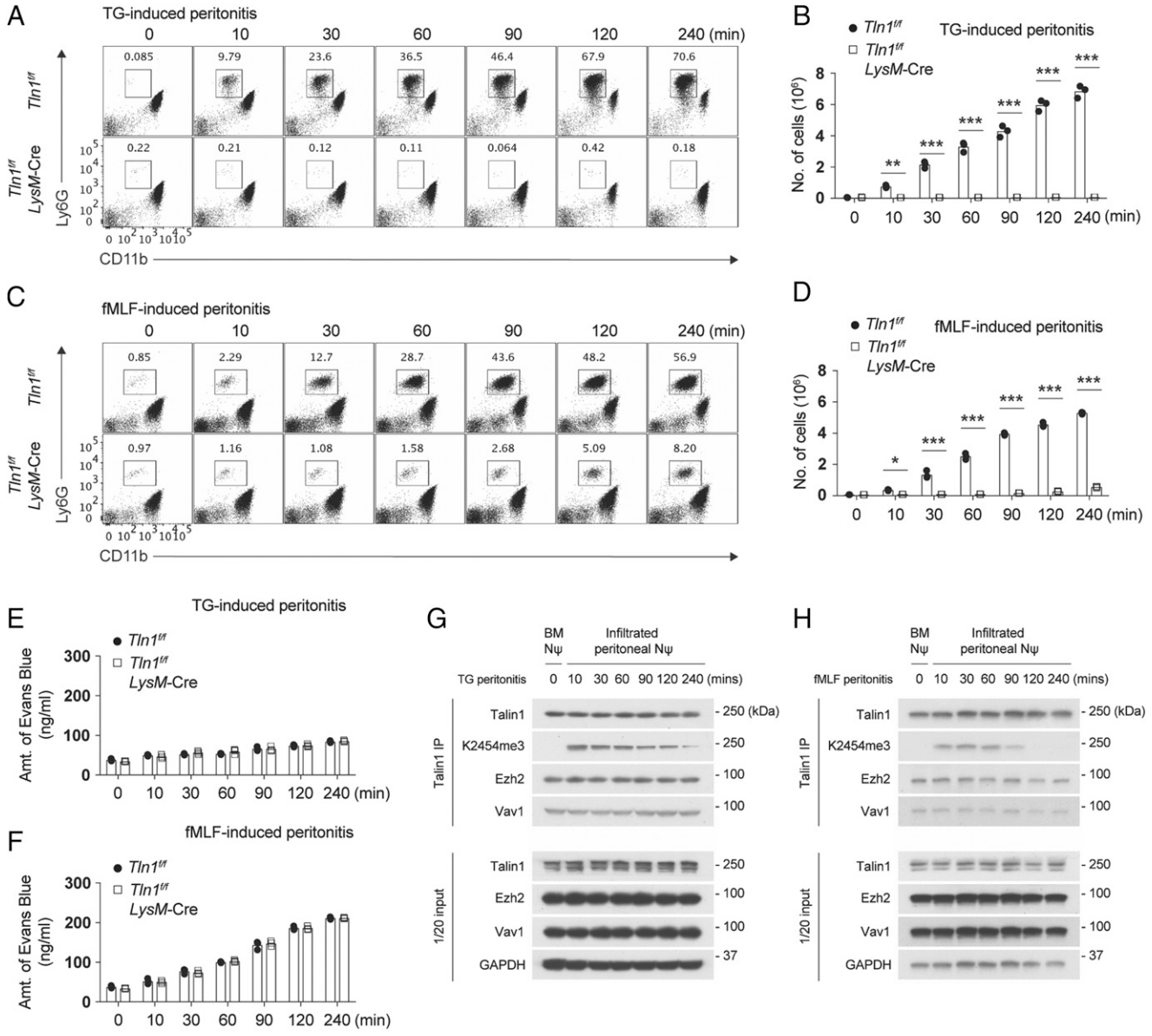

FIGURE 2. Peritonitis-induced talin1 methylation in peritoneal neutrophils. (**A**) Representative dot plots of $Ly6G^+CD11b^+$ peritoneal neutrophils at various time points following thioglycolate-induced peritonitis. Control (*Tln1$^{f/f}$*) and *Tln1$^{f/f}$LysM*-Cre mice were i.p. injected with thioglycolate, and peritoneal cells were collected at the indicated time points for flow cytometry analysis ($n = 3$ per genotype). (**B**) Absolute numbers of $Ly6G^+CD11b^+$ peritoneal neutrophils isolated from mice treated as described in (A). (**C**) Representative dot plots of $Ly6G^+CD11b^+$ peritoneal neutrophils upon fMLF-induced peritonitis. Control (*Tln1$^{f/f}$*) and *Tln1$^{f/f}$LysM*-Cre mice were i.p. injected with fMLF, and peritoneal cells were collected at the indicated time points for flow cytometry analysis ($n = 3$ per genotype). (**D**) Absolute numbers of $Ly6G^+CD11b^+$ peritoneal neutrophils isolated from mice treated as described in (C). The data shown was pregated on singlet, live cells, then $Ly6G^+CD11b^+$ neutrophils were further analyzed (A and C). (**E** and **F**) To determine the extent of vascular leakage, Evans blue dye was injected i.v. into experimental mice 30 min before inducing peritonitis. Quantification of Evans blue dye in the peritoneal cavity after i.p. injection of (E) thioglycolate or (F) fMLF, at the indicated time points, is shown ($n = 3$ per genotype). (**G** and **H**) Representative immunoblots of immunoprecipitated (IP) talin1 from purified wild-type BM neutrophils (one mouse) or infiltrated peritoneal neutrophils (one mouse [60, 90, 120, and 240 min] or pooled from two to five mice for 10- and 30-min time points to acquire sufficient numbers of cells) in (G) thioglycolate or (H) fMLF-induced peritonitis at the indicated time points. Immunoblots for Vav1 and Ezh2 represent proteins co-IP with talin1. Input samples represent one twentieth of the cell lysate used for IP. Each data point in the scatter bar graphs indicates the cell number (B and D) or the amount of Evans blue dye (E and F) from the peritoneal fluid of one mouse from each experiment. The data shown are representative of summaries of three independent experiments ($n \geq 3$ mice per genotype). *$0.01 < p \leq 0.05$, **$0.005 < p \leq 0.01$, ***$p \leq 0.005$. NΨ, neutrophils; TG, thioglycolate.

migration (5) and suggest that vascular leakage may permit marginal integrin-independent transmigration of talin1-deficient neutrophils.

Peritonitis-induced talin1/K2454 trimethylation in peritoneal neutrophils

Talin1 is functionally regulated by various PTMs (21–24). Because cytosolic K2454me3 disrupts the binding of talin1 to F-actin, leading to calpain-mediated cleavage of talin1 and adhesion turnover (25, 26), we sought to determine whether the same phenomenon also plays a role in the integrin-dependent transmigration of neutrophils across the peritoneum. For these studies, we purified wild-type peritoneal neutrophils at various time points upon induction of peritonitis with thioglycolate or fMLF and assessed the levels of talin1 trimethylation. Notably, we observed a drastic increase in the level of K2454me3 in peritoneal

neutrophils 10 min after thioglycolate (Fig. 2G) or fMLF (Fig. 2H) administration, suggesting a possible role of talin1/K2454me3 in neutrophil activation and transmigration into the peritoneal cavity. Interestingly, the abundance of K2454me3 in peritoneal neutrophils gradually decreased over time (Fig. 2G, 2H), whereas the numbers of peritoneal neutrophils increased with the induction of peritonitis (Fig. 2A–D). This result suggests that K2454me3 is likely to be transient, because it is required for the extravasation of neutrophils and, therefore, only newly infiltrated neutrophils will show high levels of K2454me3. As peritonitis progresses, the ratio of newly infiltrated neutrophils within the total population of peritoneal neutrophils decreases, hence the reduction in the K2454me3 signal (Fig. 2G, 2H). In addition, our data revealed that talin1 interacts with Vav1 and Ezh2 in neutrophils (Fig. 2G, 2H), similar to what has been shown by us earlier in dendritic cells (25), suggesting that Vav1-dependent, Ezh2-mediated trimethylation of talin1/K2454 occurs in both cell types.

Talin1 methylation promotes neutrophil transmigration across the peritoneum

To test whether K2454me3 is essential for initiating the process of neutrophil transmigration, we first transduced BM cells from *Tln1*$^{f/f}$*LysM*-Cre mice with retroviruses to express either N-terminal, GFP-fused wild-type talin1, unmethylatable talin1 variants (talin1/K2454A and talin1/K2454Q), or a methyl-mimicking talin1 variant (talin1/K2454F to mimic the bulkiness and hydrophobicity of the trimethyl group). Following transduction, talin1 variant–expressing BM stem cells were FACS sorted (for GFP expression) and adoptively transferred into lethally irradiated recipient mice to generate chimeric mice. Expression of the talin1 variants and GFP control EV in neutrophils was validated by flow cytometry analysis for intracellularly stained GFP signal (Fig. 3A, top). As controls, neutrophils from *Tln1*$^{f/f}$ and *Tln1*$^{f/f}$*LysM*-Cre mice that did not receive GFP-expressing cells are shown (Fig. 3A, top two traces from histogram). We also observed comparable levels of exogenous GFP/talin1 variants (from chimeric mice) and endogenous talin1 (*Tln1*$^{f/f}$ mice) following staining for intracellular talin1 in neutrophils from the indicated mice (Fig. 3A, bottom). Moreover, the expression of talin1 variants in hematopoietic stem cells did not affect the repopulation of neutrophils (Fig. 3B) or macrophages (Fig. 3C) in various organs 8 wk postreconstitution. To determine the effects of talin1 variants on neutrophil transmigration in our chimeric mice, we used thioglycolate-induced peritonitis because thioglycolate induced less vascular leakage and integrin-independent neutrophil infiltration than fMLF (Fig. 2). Our results showed significantly higher numbers of neutrophils expressing wild-type talin1 (K2454) or methyl-mimicking talin1 (K2454F) in the peritoneal cavity 4 h after thioglycolate injection than neutrophils expressing unmethylatable talin1 variants (Fig. 3D, 3E). These observations are in accordance with our previous in vitro studies in which we showed that unmethylatable talin1 forms very stable adhesion structures because of increased binding affinity for F-actin (25, 26). Consequently, talin1/K2454A/Q-expressing neutrophils are likely to remain tightly bound to the endothelium and are not able to extravasate into the peritoneal cavity. In contrast, talin1/K2454F may mimic talin1/K2454me3 (at least partially), thereby reducing talin1 binding to F-actin, promoting adhesion turnover, and allowing peritoneal extravasation to occur (Fig. 3D, 3E) (25, 26). The partial methyl-mimicking feature of the K2454F variant was further supported by immunoblot analysis of immunoprecipitated GFP/talin1 variants, which showed that wild-type trimethylated talin1 (K2454me3) and, to some extent, the methyl-mimicking talin1/K2454F, but not the unmethylatable variants talin1/K2454A and talin1/K2454Q, could be detected using our custom, K2454me3-specific Ab (25) (Fig. 3F).

In previous studies, we demonstrated that exogenous expression of talin1/K2454F is sufficient to rescue the migratory defect of Ezh2-deficient dendritic cells (25). To examine the involvement of Ezh2-dependent methylation of talin1 in the transmigration of neutrophils across the peritoneum, we treated control (*Tln1*$^{f/f}$) mice with the Ezh2 inhibitor GSK126 before inducing peritonitis with LPS. In this study, we used a dose of GSK126 (10 mg/kg) that is well below the tolerable range for GSK126 treatment in mice (15 or 50 mg/kg) (33, 34). Our results showed that, in the absence of LPS, the numbers of wild-type peritoneal neutrophils treated with or without GSK126 were low and comparable to the numbers of peritoneal talin1-deficient neutrophils (Fig. 3G, 3H). However, in the context of LPS-induced peritonitis, untreated *Tln1*$^{f/f}$*LysM*-Cre mice and GSK126-treated control mice both showed significantly lower numbers of neutrophils in the peritoneal cavity than untreated control mice (Fig. 3G, 3H), indicating that the transmigration of neutrophils into the peritoneal cavity is dependent upon the enzymatic activity of Ezh2, even in the presence of endogenous talin1. Collectively, our data demonstrate that Ezh2-mediated talin1/K2454me3 is required for neutrophil transmigration across the peritoneum.

A high dose of zymosan A induces integrin-independent infiltration of neutrophils

To study neutrophil transmigration in a more physiological setting, we induced peritonitis using various doses of heat-inactivated zymosan A, a glycan derived from the cell wall of yeast (35). Similar to fMLF and thioglycolate, the infiltration capacity of talin1-deficient neutrophils into the peritoneal cavity in response to low doses of zymosan A (10 and 50 μg) was compromised (Fig. 4A). A substantial increase in the number of talin1-deficient neutrophils was detected in the peritoneal cavity upon treatment with 200 μg zymosan A, but it was still significantly lower than the number of infiltrated wild-type neutrophils (Fig. 4A). Interestingly, comparable numbers of wild-type and talin1-deficient neutrophils were detected in the peritoneal cavities of mice injected with an extremely high dose of zymosan A (Fig. 4A, 500 μg), suggesting the usage of integrin-independent migration by infiltrating neutrophils into the severely inflamed peritoneal cavity. It is also likely that severe vascular leakage contributes to the extravasation of talin1-deficient neutrophils. Indeed, a dose-dependent increase of Evans blue dye in the peritoneal fluid and tissues was observed in mice treated with increasing doses of zymosan A (Fig. 4B, 4C). The amount of Evans blue dye in the peritoneal cavity was relatively low in mice treated with up to 200 μg of zymosan A but increased dramatically upon treatment with 500 μg of zymosan A (Fig. 4B, 4C) and correlated with the dramatic increase in the number of talin1-deficient neutrophils in the peritoneal cavity (Fig. 4A). These results support the concept of integrin-independent extravasation of neutrophils under severe inflammatory conditions.

Next, we induced peritonitis in our talin1-variant chimeric mice using various doses of zymosan A to examine the physiological relevance of talin1/K2454me3 in neutrophils under different grades of inflammation. With low-grade inflammation and minimal vascular leakage induced by injecting up to 200 μg of zymosan A, we observed elevated numbers of infiltrated neutrophils expressing wild-type talin1 or methyl-mimicking talin1/K2454F in the peritoneal cavity, whereas substantially lower numbers of talin1-deficient neutrophils (EV) or neutrophils expressing unmethylatable talin1 were recruited (Fig. 4D, 4E). Similar to our earlier experiments, neutrophils were detected in the severely inflamed peritoneal cavity induced by 500 μg of zymosan A regardless of the talin1 variant expressed or the methylation status of K2454 (Fig. 4D, 4E). Taken

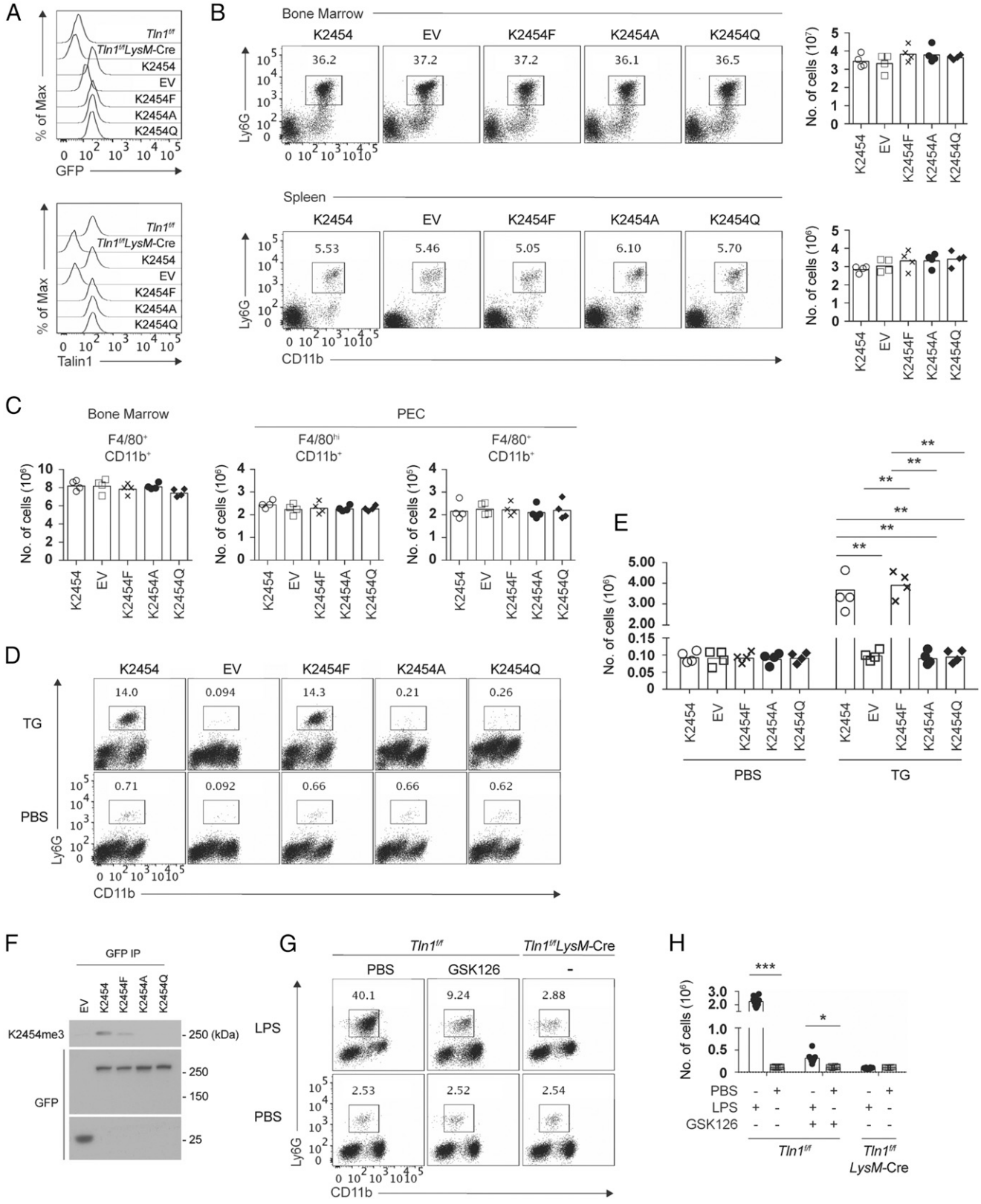

FIGURE 3. Talin1 methylation is required for neutrophil infiltration during peritonitis. (**A**) BM (CD45.2$^+$) cells isolated from 5-fluorouracil–treated *Tln1$^{f/f}$LysM*-Cre mice were transduced with retrovirus to express either GFP control EV, wild-type talin1 (K2454), talin1/K2454F, talin1/K2454A, or talin1/K2454Q and then adoptively transferred into lethally irradiated CD45.1 congenic wild-type mice. Reconstituted chimeric mice were analyzed 8 wk posttransplantation. Histograms, as determined by flow cytometry, show the expression of intracellular GFP (top) and talin1 (bottom) in the BM neutrophils of control (*Tln1$^{f/f}$*), *Tln1$^{f/f}$LysM*-Cre, or chimeric mice (indicated by K2454, EV, K2454F, K2454A, and K2454Q) (n = 3 per genotype). In this study, enhancement of GFP/talin1 signal by intracellular staining for GFP with anti-GFP, FITC-conjugated secondary Ab was required upon fixation. (**B**) Representative dot plots (left) and absolute numbers (right) of Ly6G$^+$CD11b$^+$ neutrophils from the BM and spleens of chimeric mice with myeloid cells expressing the indicated talin1 variants (n = 4 per genotype). (**C**) Absolute numbers of macrophages in the BM (gated on F4/80$^+$CD11b$^+$ cells; left scatter bar graph) and peritoneal cavity (PEC) (gated on F4/80^{hi}CD11b$^+$ or F4/80$^+$CD11b$^+$ cells; right scatter bar graphs) of chimeric *(Figure legend continues)*

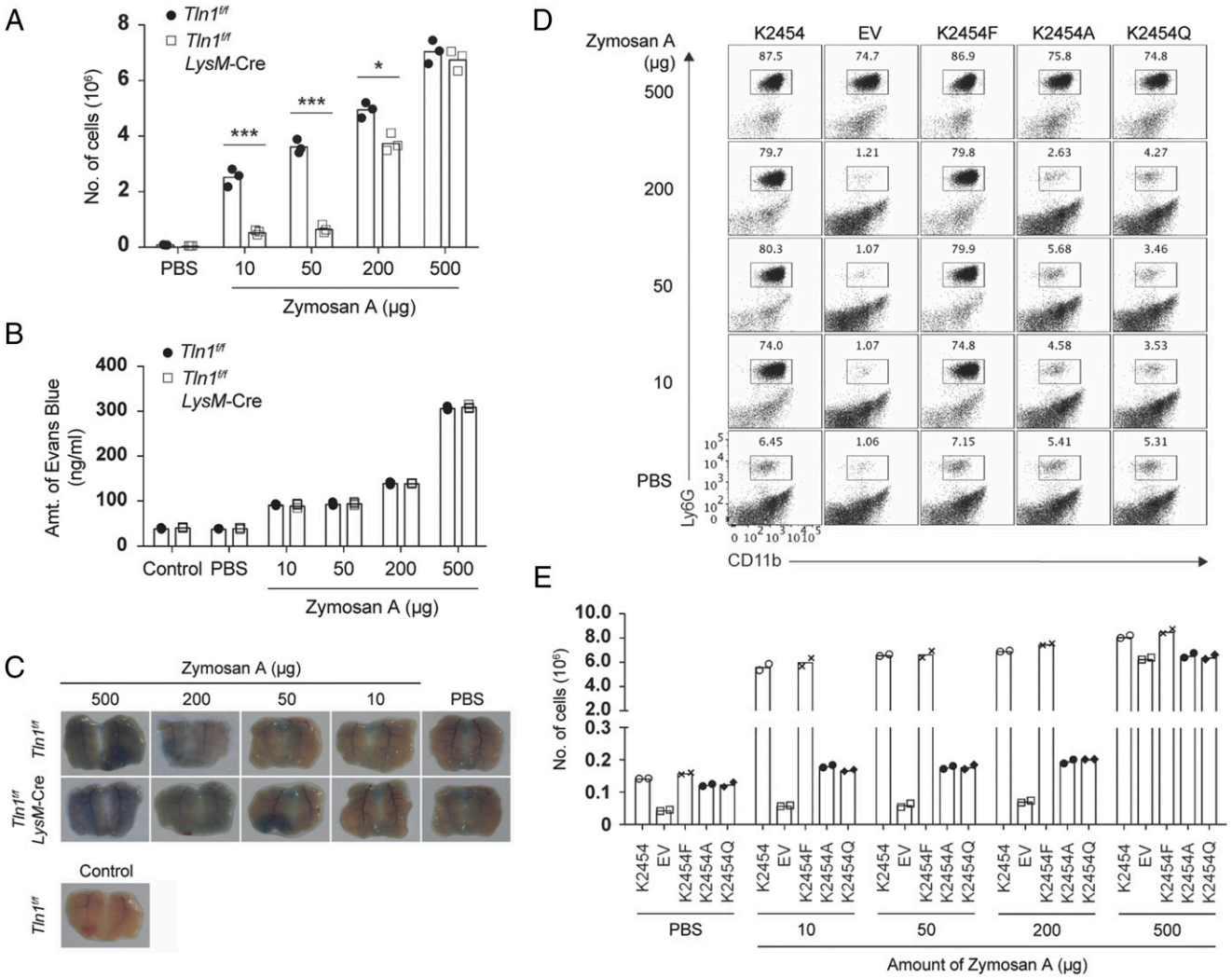

FIGURE 4. Talin1 methylation–independent extravasation of neutrophils under exaggerated inflammatory conditions. (**A**) Absolute numbers of $Ly6G^+CD11b^+$ peritoneal neutrophils. Control (*Tln1$^{f/f}$*) and *Tln1$^{f/f}$LysM*-Cre mice were i.p. injected with various amounts of zymosan A. Peritoneal cells were collected 4 h later and stained for flow cytometry analysis ($n = 3$ per genotype). (**B**) Quantification of Evans blue dye in the peritoneal cavity 4 h after i.p. injection of zymosan A ($n = 3$ per genotype). Evans blue was injected before the induction of peritonitis, as described in Fig. 2E. (**C**) Representative images of Evans blue–stained peritoneal membranes 4 h after i.p. injection of zymosan A were taken by digital camera with microimaging mode ($n = 3$ per genotype). (**D**) Representative dot plots and (**E**) absolute numbers of $Ly6G^+CD11b^+$ peritoneal neutrophils of chimeric mice with myeloid cells expressing talin1 variants (wild-type talin1 [K2454], talin1/K2454F, talin1/K2454A, talin1/K2454Q, and EV as control) 4 h after i.p. injection of zymosan A ($n = 2$ per genotype). Chimeric mice were generated as described in Fig. 3A. The data were pregated on singlet, live cells, and then $Ly6G^+CD11b^+$ neutrophils were further analyzed (A and D). Each data point in the scatter bar graphs indicates the cell number (A and E) or amount of Evans blue dye (B) from the peritoneal fluid of one mouse from each experiment. Representative or summarized data from two (D and E) or three (A–C) independent experiments are shown. $*0.01 < p \leq 0.05$, $***p \leq 0.005$.

together, our data demonstrate that Ezh2-promoted talin1 methylation is required for neutrophil extravasation into the peritoneal cavity under low to intermediate inflammatory conditions, but is dispensable at high grades of inflammation.

Inhibition of talin1 methylation attenuates LPS-induced mortality

Although a protective role for neutrophils in sepsis has recently been proposed based on results obtained in mice with complete depletion of neutrophils either by Ab treatment or diphtheria toxin receptor–mediated conditional cell ablation (36), neutrophils are generally associated with exacerbated inflammation and tissue damage upon LPS exposure or in various physiological contexts (37). Because K2454me3 of talin1 is essential for integrin-dependent neutrophil transmigration, we wondered if chimeric mice with talin1-deficient neutrophils or neutrophils expressing unmethylatable talin1 variants would be better protected against, or more susceptible to, LPS-induced mortality. Following LPS

mice ($n = 4$ per genotype). (**D**) Representative dot plots and (**E**) absolute numbers of $Ly6G^+CD11b^+$ neutrophils from chimeric mice 4 h after i.p. injection of thioglycolate ($n = 4$ per genotype). (**F**) GFP/talin1 variants were overexpressed in HEK-293T cells and immunoprecipitated (IP) with anti-GFP Abs. Immunoblots were probed with anti-talin1/K2454me3–specific Abs. (**G**) Representative dot plots and (**H**) absolute numbers of peritoneal $Ly6G^+CD11b^+$ neutrophils from PBS- or GSK126-treated control (*Tln1$^{f/f}$*) and *Tln1$^{f/f}$LysM*-Cre mice 24 h after i.p. injection of LPS ($n = 10$ per genotype). Each data point in the scatter bar graphs indicates the cell number calculated for one mouse from each experiment (B, C, E, and H). The data shown was pregated on singlet, live cells, and then $Ly6G^+CD11b^+$ neutrophils (A, B, D, E, G, and H) or the indicated macrophages (C) were further analyzed. The data shown are representative of summaries of two (F) or three (A–E, G, and H) independent experiments. $*0.01 < p \leq 0.05$, $**0.005 < p \leq 0.01$, $***p \leq 0.005$. TG, thioglycolate.

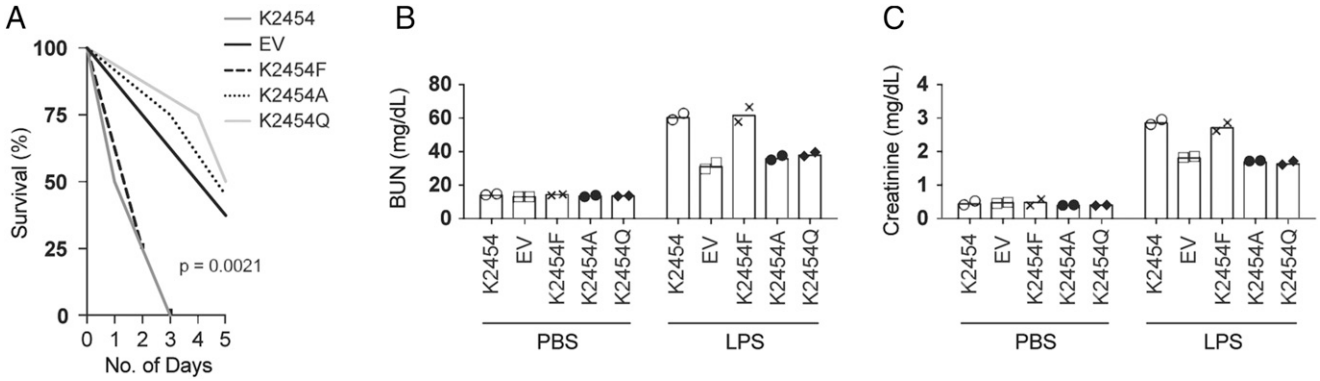

FIGURE 5. Inhibition of talin1 methylation protects against LPS-induced endotoxemia. (**A**) Kaplan–Meier survival analysis of chimeric mice with myeloid cells expressing various talin1 variants (wild-type talin1 [K2454], talin1/K2454F, talin1/K2454A, talin1/K2454Q, and EV as control) after i.p. injection of LPS (15 mg/kg body weight) ($n = 4$ per genotype). Chimeric mice were generated as described in Fig. 3A. (**B** and **C**) Quantification of BUN and creatinine in the blood of chimeric mice i.p. injected with LPS or PBS control. Peripheral blood from chimeric mice was collected 20−24 h after LPS or PBS injection. Blood leukocytes were removed by centrifugation, and the amount of BUN and creatinine was quantified by ELISA ($n = 2$ per genotype). Each data point in the scatter bar graphs indicates the amount of BUN (B) or creatinine (C) from one mouse. The data shown are representative of summaries of two independent experiments.

injection, we observed significant improvements in the survival of chimeric mice with talin1-deficient neutrophils (EV) or neutrophils expressing unmethylatable talin1 variants (K2454A and K2454Q), whereas mice with neutrophils expressing wild-type talin1 (K2454) or methyl-mimicking talin1/K2454F were more susceptible to LPS-induced mortality (Fig. 5A).

Multiorgan failure is a prominent feature of LPS-induced mortality (38, 39). This is largely due to the excessive infiltration of neutrophils into organs such as the lungs, liver, and kidneys, leading to serious organ damage (37). With this in mind, we examined the extent of organ damage by injecting LPS into our chimeric mice and measured the levels of blood metabolites such as creatinine and BUN (38, 40, 41). As expected, we detected elevated amounts of creatinine and BUN in the blood of LPS-treated mice compared with PBS-injected control mice (Fig. 5B, 5C). We also detected higher amounts of creatinine and BUN in the chimeric mice with neutrophils expressing wild-type talin1 (K2454) or talin1/K2454F than in the chimeric mice with talin1-deficient neutrophils (EV) or neutrophils expressing unmethylatable talin1/K2454A or talin1/K2454Q (Fig. 5B, 5C). These results indicate that talin1 methylation may be associated with extensive organ damage.

Similar to the extravasation of neutrophils across the peritoneum, the infiltration of neutrophils into various organs is also integrin dependent (42); therefore, we proceeded to investigate the extent of neutrophil infiltration into these organs in LPS-treated mice. Twenty to twenty-four hours after the administration of LPS into our chimeric mice, we observed markedly increased numbers of infiltrated neutrophils in the liver (Fig. 6A, 6B), kidneys (Fig. 6C, 6D), and lungs (Fig. 6E, 6F); all of which are known to be critically damaged by LPS-induced endotoxemia (38–41). We also observed the increased translocation of neutrophils into the airspace of the lungs of LPS-treated chimeric mice as determined in BALF, compared with PBS-injected mice, whereas the numbers of alveolar macrophages ($F4/80^+$ $Ly6G^-$) remained constant under all experimental conditions (Fig. 6G, 6H). Similar to our earlier observations that talin1/K2454me3 is essential for integrin-dependent neutrophil transmigration across the endothelium (Fig. 3), we consistently detected higher numbers of wild-type neutrophils or neutrophils expressing methyl-mimicking talin1/K2454F in various organs and the BALF of LPS-treated mice than what was quantified in mice with talin1-deficient neutrophils or neutrophils expressing unmethylatable talin1/K2454A or talin1/K2454Q (Fig. 6B, 6D, 6F, 6H). The numbers of neutrophils in the various organs and BALF of our chimeric mice also positively correlated with the increased mortality caused by LPS-induced endotoxemia (Fig. 5A). Furthermore, the number of neutrophils in the peripheral blood inversely correlated with the numbers of BALF-isolated neutrophils from the aforementioned chimeric mice (Fig. 6I, 6J). Collectively, these data suggest an important role for talin1 methylation in the transmigration of neutrophils from the blood into various organs in vivo during LPS-induced endotoxemia.

Discussion

In this study, we have demonstrated that Ezh2-mediated talin1 methylation plays an important role in promoting the transmigration of neutrophils across the peritoneum in several animal models of sterile peritonitis. Furthermore, the inhibition of Ezh2-mediated talin1 methylation greatly reduces the number of infiltrating neutrophils into the peritoneal cavity as well as multiple vital organs, which can significantly improve the survival rate of mice treated with a lethal dose of LPS. These results are consistent with the general consensus that neutrophils aggravate inflammation and enhance the tissue damage that is frequently associated with dysregulated neutrophil activation or neutrophil extracellular traps (43, 44). Although neutrophils can efficiently eliminate invading pathogens through various defense mechanisms, some neutrophil products and the aforementioned dysregulation of neutrophil functions could be detrimental to the host in LPS-induced endotoxemia. In our experimental model, the reduced infiltration of talin1-deficient neutrophils or neutrophils expressing unmethylatable talin1 did not increase LPS-induced mortality, which is in contrast to what was observed in neutrophil-depleted mice (36). This is likely due to the incomplete blockage of the migration of these neutrophils, resulting in numbers of infiltrated neutrophils in the peritoneal cavity and/or organs that are sufficient to confer protection either through myeloperoxidase-dependent mechanisms or pathways related to macrophage-dependent clearance of apoptotic neutrophils to control and resolve the inflammation (36, 45).

We also observed a prominent increase in the abundance of talin1/K2454me3 in peritoneal neutrophils during peritonitis, but not in BM neutrophils, suggesting an association of the methylation event with neutrophil activation and integrin-dependent migration of neutrophils into the peritoneal cavity as peritonitis progresses. Interestingly, whereas neutrophils accumulated in the peritoneal

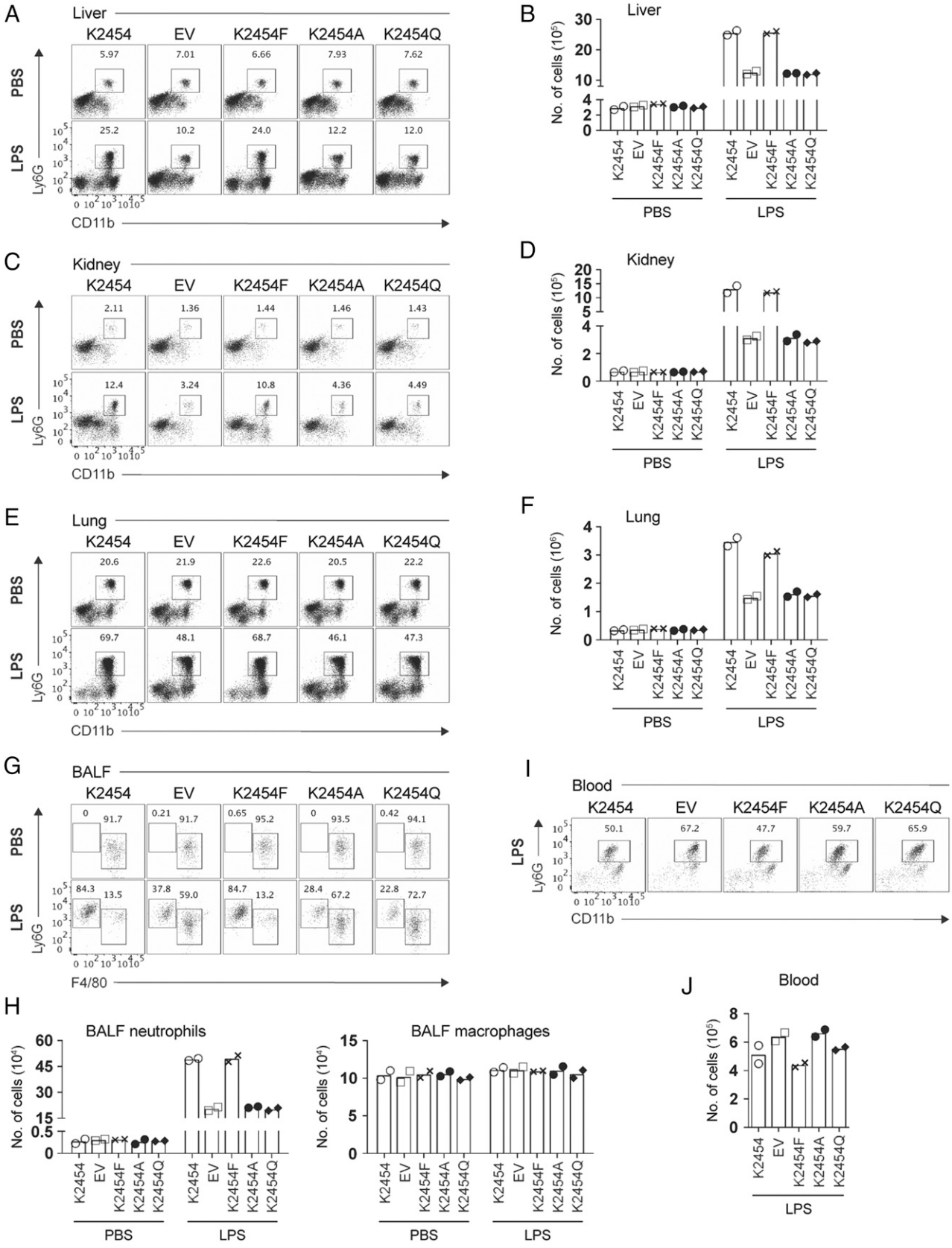

FIGURE 6. Talin1 methylation promotes neutrophil infiltration and organ damage during LPS-induced endotoxemia. Representative dot plots (**A**, **C**, **E**, **G**, and **I**) and absolute numbers of neutrophils (**B**, **D**, **F**, **H**, and **J**) isolated from the liver (A and B), kidney (C and D), lung (E and F), BALF (G and H), and peripheral blood (I and J) of chimeric mice with myeloid cells expressing talin1 variants (wild-type talin1 [K2454], talin1/K2454F, talin1/K2454A, talin1/K2454Q, and EV as control) (n = 2 per genotype). Chimeric mice were generated as described in Fig. 3A. Organs and BALF were collected 20−24 h after i.p. injection of LPS (15 mg/kg body weight) or PBS control. Organs were processed, and cells were stained for flow cytometry analysis. The data were pregated on singlet, live cells. Neutrophils were defined as $Ly6G^+$ or $Ly6G^+CD11b^+$ cells (B, D, F, H, and J). Alveolar macrophages were defined as $F4/80^+Ly6G^-$ cells [(H), right]. Each point in the scatter bar graphs indicates the cell number calculated from one experiment (B, D, F, H, and J). The data shown are representative of summaries of two independent experiments.

cavity, the intensity of talin1 methylation decreased gradually over time. This suggests that the methylation of talin1 at K2454 is likely to be transient, with the methyl group being actively removed by demethylase(s). Methylated talin1 could also be degraded over time, because we have previously reported that methyl-mimicking talin1/K2454F promotes talin1 cleavage (26). Moreover, although i.p. administration of thioglycolate or fMLF promotes the successive recruitment of neutrophils over a period of 4 h, only newly infiltrated neutrophils would express high levels of talin1/K2454me3. Therefore, as peritonitis progresses, the proportion of newly infiltrated neutrophils within the total peritoneal neutrophil population would be reduced, resulting in reduced (diluted) talin1/K2454me3 signal. Alternatively, increased vascular leakage, in conjunction with increased numbers of infiltrating neutrophils through integrin-independent mechanisms, could also contribute to the reduced talin1/K2454me3 signal. In fact, pronounced vascular leakage and integrin-independent migration of control and talin1-deficient neutrophils were observed at high doses of zymosan A (500 μg). However, peritonitis induced by fMLF or thioglycolate in our current experimental setting did not promote substantial integrin-independent infiltration of talin1-deficient neutrophils into the peritoneal cavity. Thus, we conclude that the talin1 methylation signal in peritoneal neutrophils is transient.

ABS3, where the Ezh2-mediated talin1/K2454 methylation site is located (25), is believed to be critical for the initiation of F-actin binding (13, 46). We reported previously that the trimethylation of talin1/K2454 (K2454me3), or using a mutant talin1 that substitutes Lys2454 with the methyl-mimicking amino acid phenylalanine (K2454F), disrupts talin1 binding to F-actin. In contrast, substituting Lys2454 with unmethylatable residues alanine or glutamine (K2454A or Q) results in strong talin1 binding to F-actin (25). Consequently, expression of the methyl-mimicking talin1 mutant promotes adhesion turnover, whereas expression of either of the unmethylatable talin1 mutants results in very stable FAs (25, 26). It is currently unclear whether talin1/K2454me3 regulates adhesion turnover by affecting molecules associated with adhesion structures other than ABS3-associated F-actin. However, we have demonstrated unperturbed interactions of the talin1 methylation variants with CD11b and CD29 in a separate study conducted using BM-derived dendritic cells (T.J.F. Lim and I-H. Su, unpublished observations). Taken together, we predict that Ezh2-mediated talin1 methylation is unlikely to interfere with the binding of talin1 to integrins or other FA proteins in the context of neutrophil transmigration.

The expression levels of our exogenous talin1 variants are largely comparable to the levels of endogenous talin1 and exhibit perinuclear localization (26), suggesting that talin1, regardless of its origin or methylation status, can form autoinhibitory configurations and does not constitutively contribute to adhesion turnover. This is in accordance with our current data showing that the distributions of wild-type talin1 and talin1 variant–expressing neutrophils and macrophages are comparable in the BM of chimeric mice. However, once activated, neutrophils arrest and crawl on the inflamed endothelium to reach the ideal vascular emigration site before initiating the process of transmigration (47). At this stage, talin1/K2454 methylation is likely to be required for adhesion turnover. Indeed, similar numbers of infiltrated peritoneal neutrophils expressing wild-type talin1 (K2454) or the methyl-mimicking talin1/K2454F suggest that adhesion turnover is comparable between these neutrophils. It is possible that the talin1 methylation–induced dissociation of F-actin at ABS3 (25) is highly efficient; as such, the half-lives of adhesion structures associated with wild-type talin1 and talin1-K2454F may be comparable. We also cannot rule out the possibility that the methyl-mimicking residue phenylalanine (F) is not a complete substitute for the trimethylated lysine residue. Currently, there is no suitable way to estimate the efficiency of in vivo talin1 methylation. However, our data suggest that the substitution of lysine (K) with phenylalanine (F) may not fully mimic trimethylation, as indicated by the reduced detection of talin1/K2454F using the anti-methyl/talin1–specific Ab that was raised against K2454me3 peptides (25). Thus, we do not expect talin1/K2454F-expressing neutrophils to exhibit enhanced or defective extravasation capabilities.

Aside from neutrophils, macrophages were also talin1 deficient or expressed various talin1 variants in our BM chimeric mice; however, integrin-dependent migration and/or extravasation is not required for the localization of tissue-resident, large peritoneal macrophages (48). As for the monocyte-derived small peritoneal macrophages, the deletion of *loxP*-flanked genes by *Lyz2* promoter–driven Cre recombinase is not as efficient in monocytes as it is in neutrophils and macrophages (28). It is likely that endogenous talin1 is still expressed in blood monocytes during their transmigration into the peritoneal cavity before terminally differentiating into macrophages. Therefore, it is unlikely that talin1 methylation regulates the effector functions of other myeloid cells besides neutrophils in our experimental setting of LPS-induced endotoxemia. Collectively, our study reveals a physiological role for talin1 methylation in sterile peritonitis. Based on these results, we predict that inhibiting talin methylation, such as by blocking the lysine methyltransferase Ezh2, may be a valid strategy for treating inflammatory disorders associated with neutrophils. This novel mechanism is likely to regulate immune responses mediated by different immune cells and have broad relevance to various disease conditions.

Acknowledgments

We thank Dr. Brian G. Petrich (Emory University) for providing the talin1-conditional knockout mice and A*STAR Biological Resource Centre for providing the *LysM*-Cre knock-in mice. We also thank A. Sullivan from Obrizus Communications for critical reading and editing the manuscript.

Disclosures

The authors have no financial conflicts of interest.

References

1. Ley, K., C. Laudanna, M. I. Cybulsky, and S. Nourshargh. 2007. Getting to the site of inflammation: the leukocyte adhesion cascade updated. *Nat. Rev. Immunol.* 7: 678–689.
2. Yago, T., B. G. Petrich, N. Zhang, Z. Liu, B. Shao, M. H. Ginsberg, and R. P. McEver. 2015. Blocking neutrophil integrin activation prevents ischemia-reperfusion injury. *J. Exp. Med.* 212: 1267–1281.
3. McEver, R. P., and C. Zhu. 2010. Rolling cell adhesion. *Annu. Rev. Cell Dev. Biol.* 26: 363–396.
4. Yago, T., B. Shao, J. J. Miner, L. Yao, A. G. Klopocki, K. Maeda, K. M. Coggeshall, and R. P. McEver. 2010. E-selectin engages PSGL-1 and CD44 through a common signaling pathway to induce integrin alphaLbeta2-mediated slow leukocyte rolling. *Blood* 116: 485–494.
5. Lefort, C. T., J. Rossaint, M. Moser, B. G. Petrich, A. Zarbock, S. J. Monkley, D. R. Critchley, M. H. Ginsberg, R. Fässler, and K. Ley. 2012. Distinct roles for talin-1 and kindlin-3 in LFA-1 extension and affinity regulation. *Blood* 119: 4275–4282.
6. Li, H., Y. Deng, K. Sun, H. Yang, J. Liu, M. Wang, Z. Zhang, J. Lin, C. Wu, Z. Wei, and C. Yu. 2017. Structural basis of kindlin-mediated integrin recognition and activation. *Proc. Natl. Acad. Sci. USA* 114: 9349–9354.
7. Muller, W. A. 2011. Mechanisms of leukocyte transendothelial migration. *Annu. Rev. Pathol.* 6: 323–344.
8. Hamadi, A., M. Bouali, M. Dontenwill, H. Stoeckel, K. Takeda, and P. Rondé. 2005. Regulation of focal adhesion dynamics and disassembly by phosphorylation of FAK at tyrosine 397. *J. Cell Sci.* 118: 4415–4425.
9. Abe, A., K. Saeki, T. Yasunaga, and T. Wakabayashi. 2000. Acetylation at the N-terminus of actin strengthens weak interaction between actin and myosin. *Biochem. Biophys. Res. Commun.* 268: 14–19.
10. Nyman, T., H. Schüler, E. Korenbaum, C. E. Schutt, R. Karlsson, and U. Lindberg. 2002. The role of MeH73 in actin polymerization and ATP hydrolysis. *J. Mol. Biol.* 317: 577–589.
11. Huszar, G., and M. Elzinga. 1972. Homologous methylated and nonmethylated histidine peptides in skeletal and cardiac myosins. *J. Biol. Chem.* 247: 745–753.

12. Calderwood, D. A., I. D. Campbell, and D. R. Critchley. 2013. Talins and kindlins: partners in integrin-mediated adhesion. *Nat. Rev. Mol. Cell Biol.* 14: 503–517.
13. Goksoy, E., Y. Q. Ma, X. Wang, X. Kong, D. Perera, E. F. Plow, and J. Qin. 2008. Structural basis for the autoinhibition of talin in regulating integrin activation. *Mol. Cell* 31: 124–133.
14. Zhang, H., Y.-C. Chang, Q. Huang, M. L. Brennan, and J. Wu. 2016. Structural and functional analysis of a talin triple-domain module suggests an alternative talin autoinhibitory configuration. *Structure* 24: 721–729.
15. Ye, X., M. A. McLean, and S. G. Sligar. 2016. Phosphatidylinositol 4,5-bisphosphate modulates the affinity of talin-1 for phospholipid bilayers and activates its autoinhibited form. *Biochemistry* 55: 5038–5048.
16. Chang, Y.-C., H. Zhang, J. Franco-Barraza, M. L. Brennan, T. Patel, E. Cukierman, and J. Wu. 2014. Structural and mechanistic insights into the recruitment of talin by RIAM in integrin signaling. *Structure* 22: 1810–1820.
17. Yu, C. H., N. B. M. Rafiq, F. Cao, Y. Zhou, A. Krishnasamy, K. H. Biswas, A. Ravasio, Z. Chen, Y.-H. Wang, K. Kawauchi, et al. 2015. Integrin-beta3 clusters recruit clathrin-mediated endocytic machinery in the absence of traction force. *Nat. Commun.* 6: 8672.
18. Sun, Z., H.-Y. Tseng, S. Tan, F. Senger, L. Kurzawa, D. Dedden, N. Mizuno, A. A. Wasik, M. Thery, A. R. Dunn, and R. Fässler. 2016. Kank2 activates talin, reduces force transduction across integrins and induces central adhesion formation. *Nat. Cell Biol.* 18: 941–953.
19. Bouchet, B. P., R. E. Gough, Y.-C. Ammon, D. van de Willige, H. Post, G. Jacquemet, A. M. Altelaar, A. J. R. Heck, B. T. Goult, and A. Akhmanova. 2016. Talin-KANK1 interaction controls the recruitment of cortical microtubule stabilizing complexes to focal adhesions. *eLife* 5: e18124.
20. Boras, M., S. Volmering, A. Bokemeyer, J. Rossaint, H. Block, B. Bardel, V. Van Marck, B. Heitplatz, S. Kliche, A. Reinhold, et al. 2017. Skap2 is required for β_2 integrin-mediated neutrophil recruitment and functions. *J. Exp. Med.* 214: 851–874.
21. Franco, S. J., M. A. Rodgers, B. J. Perrin, J. Han, D. A. Bennin, D. R. Critchley, and A. Huttenlocher. 2004. Calpain-mediated proteolysis of talin regulates adhesion dynamics. *Nat. Cell Biol.* 6: 977–983.
22. Huang, C., Z. Rajfur, N. Yousefi, Z. Chen, K. Jacobson, and M. H. Ginsberg. 2009. Talin phosphorylation by Cdk5 regulates Smurf1-mediated talin head ubiquitylation and cell migration. *Nat. Cell Biol.* 11: 624–630.
23. Zhang, F., S. Saha, and A. Kashina. 2012. Arginylation-dependent regulation of a proteolytic product of talin is essential for cell-cell adhesion. *J. Cell Biol.* 197: 819–836.
24. Jin, J.-K., P.-C. Tien, C.-J. Cheng, J. H. Song, C. Huang, S.-H. Lin, and G. E. Gallick. 2015. Talin1 phosphorylation activates β1 integrins: a novel mechanism to promote prostate cancer bone metastasis. *Oncogene* 34: 1811–1821.
25. Gunawan, M., N. Venkatesan, J. T. Loh, J. F. Wong, H. Berger, W. H. Neo, L. Y. J. Li, M. K. La Win, Y. H. Yau, T. Guo, et al. 2015. The methyltransferase Ezh2 controls cell adhesion and migration through direct methylation of the extranuclear regulatory protein talin. *Nat. Immunol.* 16: 505–516.
26. Venkatesan, N., J. F. Wong, K. P. Tan, H. H. Chung, Y. H. Yau, E. Cukuroglu, A. Allahverdi, L. Nordenskiöld, J. Göke, S. Geifman-Shochat, et al. 2018. EZH2 promotes neoplastic transformation through VAV interaction-dependent extranuclear mechanisms. *Oncogene* 37: 461–477.
27. Petrich, B. G., P. Marchese, Z. M. Ruggeri, S. Spiess, R. A. M. Weichert, F. Ye, R. Tiedt, R. C. Skoda, S. J. Monkley, D. R. Critchley, and M. H. Ginsberg. 2007. Talin is required for integrin-mediated platelet function in hemostasis and thrombosis. *J. Exp. Med.* 204: 3103–3111.
28. Clausen, B. E., C. Burkhardt, W. Reith, R. Renkawitz, and I. Förster. 1999. Conditional gene targeting in macrophages and granulocytes using LysMcre mice. *Transgenic Res.* 8: 265–277.
29. Lim, J. F., H. Berger, and I. H. Su. 2016. Isolation and activation of murine lymphocytes. *J. Vis. Exp.* DOI: 10.3791/54596.
30. Vono, M., A. Lin, A. Norrby-Teglund, R. A. Koup, F. Liang, and K. Loré. 2017. Neutrophils acquire the capacity for antigen presentation to memory $CD4^+$ T cells in vitro and ex vivo. *Blood* 129: 1991–2001.
31. Sandilands, G. P., J. McCrae, K. Hill, M. Perry, and D. Baxter. 2006. Major histocompatibility complex class II (DR) antigen and costimulatory molecules on in vitro and in vivo activated human polymorphonuclear neutrophils. *Immunology* 119: 562–571.
32. Phillipson, M., B. Heit, S. A. Parsons, B. Petri, S. C. Mullaly, P. Colarusso, R. M. Gower, G. Neely, S. I. Simon, and P. Kubes. 2009. Vav1 is essential for mechanotactic crawling and migration of neutrophils out of the inflamed microvasculature. *J. Immunol.* 182: 6870–6878.
33. McCabe, M. T., H. M. Ott, G. Ganji, S. Korenchuk, C. Thompson, G. S. Van Aller, Y. Liu, A. P. Graves, A. Della Pietra, III, E. Diaz, et al. 2012. EZH2 inhibition as a therapeutic strategy for lymphoma with EZH2-activating mutations. *Nature* 492: 108–112.
34. Dudakovic, A., E. T. Camilleri, S. M. Riester, C. R. Paradise, M. Gluscevic, T. M. O'Toole, R. Thaler, J. M. Evans, H. Yan, M. Subramaniam, et al. 2016. Enhancer of zeste homolog 2 inhibition stimulates bone formation and mitigates bone loss caused by ovariectomy in skeletally mature mice. *J. Biol. Chem.* 291: 24594–24606.
35. Cash, J. L., G. E. White, and D. R. Greaves. 2009. Chapter 17. Zymosan-induced peritonitis as a simple experimental system for the study of inflammation. *Methods Enzymol.* 461: 379–396.
36. Reber, L. L., C. M. Gillis, P. Starkl, F. Jönsson, R. Sibilano, T. Marichal, N. Gaudenzio, M. Bérard, S. Rogalla, C. H. Contag, et al. 2017. Neutrophil myeloperoxidase diminishes the toxic effects and mortality induced by lipopolysaccharide. *J. Exp. Med.* 214: 1249–1258.
37. Brown, K. A., S. D. Brain, J. D. Pearson, J. D. Edgeworth, S. M. Lewis, and D. F. Treacher. 2006. Neutrophils in development of multiple organ failure in sepsis. *Lancet* 368: 157–169.
38. Cunningham, P. N., H. M. Dyanov, P. Park, J. Wang, K. A. Newell, and R. J. Quigg. 2002. Acute renal failure in endotoxemia is caused by TNF acting directly on TNF receptor-1 in kidney. *J. Immunol.* 168: 5817–5823.
39. Bhargava, R., C. J. Altmann, A. Andres-Hernando, R. G. Webb, K. Okamura, Y. Yang, S. Falk, E. P. Schmidt, and S. Faubel. 2013. Acute lung injury and acute kidney injury are established by four hours in experimental sepsis and are improved with pre, but not post, sepsis administration of TNF-α antibodies. *PLoS One* 8: e79037.
40. Cunningham, P. N., Y. Wang, R. Guo, G. He, and R. J. Quigg. 2004. Role of Toll-like receptor 4 in endotoxin-induced acute renal failure. *J. Immunol.* 172: 2629–2635.
41. Doi, K., A. Leelahavanichkul, P. S. T. Yuen, and R. A. Star. 2009. Animal models of sepsis and sepsis-induced kidney injury. *J. Clin. Invest.* 119: 2868–2878.
42. Komura, K., Y. Iwata, F. Ogawa, A. Yoshizaki, T. Yamaoka, Y. Akiyama, T. Hara, M. Hasegawa, M. Fujimoto, and S. Sato. 2009. Low zone tolerance requires ICAM-1 expression to limit contact hypersensitivity elicitation. *J. Invest. Dermatol.* 129: 2661–2667.
43. Czaikoski, P. G., J. M. S. C. Mota, D. C. Nascimento, F. Sônego, F. V. S. Castanheira, P. H. Melo, G. T. Scortegagna, R. L. Silva, R. Barroso-Sousa, F. O. Souto, et al. 2016. Neutrophil extracellular traps induce organ damage during experimental and clinical sepsis. *PLoS One* 11: e0148142.
44. McDonald, B., R. P. Davis, S.-J. Kim, M. Tse, C. T. Esmon, E. Kolaczkowska, and C. N. Jenne. 2017. Platelets and neutrophil extracellular traps collaborate to promote intravascular coagulation during sepsis in mice. *Blood* 129: 1357–1367.
45. Greenlee-Wacker, M. C. 2016. Clearance of apoptotic neutrophils and resolution of inflammation. *Immunol. Rev.* 273: 357–370.
46. Atherton, P., B. Stutchbury, D.-Y. Wang, D. Jethwa, R. Tsang, E. Meiler-Rodriguez, P. Wang, N. Bate, R. Zent, I. L. Barsukov, et al. 2015. Vinculin controls talin engagement with the actomyosin machinery. *Nat. Commun.* 6: 10038.
47. Proebstl, D., M. B. Voisin, A. Woodfin, J. Whiteford, F. D'Acquisto, G. E. Jones, D. Rowe, and S. Nourshargh. 2012. Pericytes support neutrophil subendothelial cell crawling and breaching of venular walls in vivo. *J. Exp. Med.* 209: 1219–1234.
48. Ghosn, E. E. B., A. A. Cassado, G. R. Govoni, T. Fukuhara, Y. Yang, D. M. Monack, K. R. Bortoluci, S. R. Almeida, L. A. Herzenberg, and L. A. Herzenberg. 2010. Two physically, functionally, and developmentally distinct peritoneal macrophage subsets. *Proc. Natl. Acad. Sci. USA* 107: 2568–2573.